p34^{cdc2} are used to precipitate p34^{cdc2}-containing complexes from cell extracts, a number of bands are detected (*27*). Moreover, it has been proposed that p34^{cdc2} might participate in a number of different complexes (*28*). One of them might include the unknown Ca^{2+}-regulatory component.

REFERENCES AND NOTES

1. Y. Masui and C. Markert, *J. Exp. Zool.* **177**, 129 (1971); T. Kishimoto and H. Kanatani, *Nature* **260**, 321 (1976); M. Dorée, G. Peaucellier, A. Picard, *Dev. Biol.* **99**, 489 (1983); A. Picard, G. Peaucellier, F. Le Bouffant, C. Le Peuch, M. Dorée, *ibid.* **109**, 311 (1985); A. Picard *et al.*, *Dev. Growth Differ.* **29**, 93 (1987); J. Gerhart, M. Wu, M. Kirschner, *J. Cell Biol.* **98**, 1247 (1984).
2. J. C. Labbé *et al.*, *EMBO J.* **8**, 3053 (1989).
3. J. C. Labbé, M. Lee, P. Nurse, A. Picard, M. Dorée, *Nature* **335**, 251 (1988).
4. J. C. Labbé *et al.*, *Cell* **57**, 253 (1989).
5. D. Arion, L. Meijer, L. Brizuela, D. Beach, *ibid.* **55**, 371 (1988).
6. J. Gautier, C. J. Norbury, M. Lohka, P. Nurse, J. Maller, *ibid.* **54**, 433 (1988).
7. W. G. Dunphy, L. Brizuela, D. Beach, J. Newport, *ibid.*, p. 423.
8. Abbreviations for the amino acid residues are as follows: A, Ala; C, Cys; D, Asp; E, Glu; F, Phe; G, Gly; H, His; I, Ile; K, Lys; L, Leu; M, Met; N, Asn; P, Pro; Q, Gln; R, Arg; S, Ser; T, Thr; V, Val; W, Trp; and Y, Tyr.
9. C. J. Norbury and P. Nurse, *Biochim. Biophys. Acta* **989**, 85 (1989).
10. D. Epel, *Calcium and Cell Functions*, W. Y. Cheung, Ed. (Academic Press, New York, 1982), vol. 2, p. 355.
11. A. Picard and M. Dorée, *Exp. Cell Res.* **145**, 325 (1983); A. Eisen and G. Reynolds, *J. Cell Biol.* **99**, 1878 (1984); R. J. Cork, M. F. Cicirelli, R. K. Robinson, *Dev. Biol.* **121**, 41 (1987); M. F. Cicirelli and L. D. Smith, *ibid.*, p. 48; H. J. Witchell and R. A. Steinhardt, *J. Cell Biol.* **107**, 172a (1988).
12. A. Toh-e, K. Tanaka, Y. Uenoso, R. B. Wickner, *Mol. Gen. Genet.* **214**, 162 (1988).
13. R. Miledi, *Proc. R. Soc. London* **215**, 491 (1982).
14. M. E. Barish, *J. Physiol. (London)* **342**, 309 (1983).
15. R. Miledi and I. Parker, *ibid.* **357**, 173 (1984).
16. N. Dascal, B. Gillo, Y. Lass, *ibid.* **366**, 299 (1985).
17. P. Lory, J. C. Cavadore, M. Dorée, unpublished results.
18. N. Dascal, T. P. Snutch, H. Lubbert, N. R. Davidson, H. A. Lester, *Science* **231**, 1147 (1986).
19. L. Brizuela, G. Draetta, D. Beach, *EMBO J.* **6**, 3507 (1987).
20. G. Draetta, L. Brizuela, J. Potashkin, D. Beach, *Cell* **50**, 319 (1987).
21. The PSTAIR peptide was microinjected into *Xenopus* or *Marthasterias* oocytes to give an intracellular concentration of 100 or 400 μM, respectively. After 15 min, homogenates were prepared from PSTAIR peptide–injected or noninjected oocytes by crushing ten oocytes in 300 μl (*Xenopus*) or 10 μl (*Marthasterias*) of a buffer containing 50 mM β-glycerophosphate, 15 mM EGTA, 10 mM $MgCl_2$, and 1 mM dithiothreitol (*p*H 7.3). Histone H1 kinase was measured in crude extracts [J. C. Labbé, A. Picard, E. Karsenti, M. Dorée, *Dev. Biol.* **127**, 157 (1988)]. An additional experiment was performed in starfish only by microinjecting 3 μM p13^{suc1} (intracellular concentration) before injection of the PSTAIR peptide. Each experiment was performed in triplicate with identical results. The p13^{suc1} protein was purified from a strain of *Escherichia coli* expressing high levels of the yeast protein in a soluble form [S. Moreno, J. Hayles, P. Nurse, *Cell* **58**, 361 (1989)]. It was purified to apparent homogeneity by gel filtration and ion-exchange chromatography, and by taking advantage of its thermostability.
22. A. Dalcq, *Biol. Rev. Camb. Philos. Soc.* **126**, 291 (1928).
23. R. B. Silver, *Dev. Biol.* **131**, 11 (1989).
24. R. A. Steinhart and J. Alderton, *Nature* **332**, 364 (1988).
25. J. Twigg, R. Patel, M. Whitaker, *ibid.*, p. 366.
26. D. H. McLennan, K. P. Campbell, R. A. F. Reithmeier, in *Calcium and Cell Function*, A. Martonosi, Ed. (Academic Press, New York, 1983), vol. 4, p. 151; P. Volpe *et al.*, *Proc. Natl. Acad. Sci. U.S.A.* **85**, 1091 (1988); J. H. Henson *et al.*, *J. Cell Biol.* **109**, 149 (1989); G. Grynkiewwicz, M. Poenie, R. Y. Tsien, *J. Biol. Chem.* **260**, 3440 (1985).
27. G. Draetta *et al.*, *Nature* **336**, 738 (1988).
28. L. J. Cisek and J. L. Corden, *ibid.* **339**, 679 (1989).
29. B. Calas, J. Mery, J. Parello, *Tetrahedron* **41**, 5331 (1985).
30. H. Hiramoto, *Exp. Cell Res.* **87**, 403 (1974).
31. J. C. Bernengo, F. Lemteri-Chlieh, C. Ojeda, N. Platonov, *J. Physiol. (London)*, in press; N. Platonov, thesis, University of Besançon, France (1989).

2 October 1989; accepted 28 November 1989

Far-Red Radiation Reflected from Adjacent Leaves: An Early Signal of Competition in Plant Canopies

CARLOS L. BALLARÉ, ANA L. SCOPEL, RODOLFO A. SÁNCHEZ

When individual seedlings of *Datura ferox* and *Sinapis alba* were transferred to populations formed by plants of similar stature, they responded with an increase in the rate of stem elongation. The reaction was detected within 3 days after transplanting and occurred well before shading among neighbors became important. This rapid response, which may be crucial for success in the competition for light, was reduced or abolished when individual internodes were "blinded" to the far-red radiation scattered by the surrounding seedlings. These results show the operation of a localized, photomorphogenetic control of stem elongation that may play a central role in the plastic adjustment of plants during the early stages of canopy development.

ONE OF THE MOST STRIKING CHARacteristics of higher plants is their capacity to react to the presence of neighbors with changes in the pattern of morphological development. This is documented by a large number of descriptive studies, but few ecological experiments have been conducted at a sufficiently reductionist level to establish the precise nature of the morphogenetic signals (*1, 2*).

A classic example of morphological plasticity is the redistribution of growth toward stem elongation exhibited by plants of many species when growing in dense populations (*1*). Several factors of the aboveground environment that may influence elongation, such as light intensity and spectral distribution, air movement, air humidity and temperature, are substantially altered when the number of plants per unit area increases (*3*). The spectral distribution of radiation, particularly the ratio of red (R) to far-red (FR) wavelength bands (R:FR), is now widely accepted to be a powerful environmental signal for plants growing in the lower strata of established canopies (*4*). Perception of a low R:FR balance by phytochrome, a photochromic plant pigment, may trigger mechanisms whereby these plants react to shading, accelerating stem elongation (shade-avoidance reactions). This idea is supported by (i) spectroradiometric studies showing that light filtered through a leaf canopy has a low R:FR ratio due to preferential absorption of R light by chlorophyll (*5*) and (ii) physiological studies with isolated plants in which light conditions simulated those experienced by heavily shaded individuals (*6*).

Recent analysis of the growth of plants in even-aged populations revealed, however, that the stems start exhibiting increased rates of elongation well before the leaves become shaded, and thus before they experience the R-impoverished light that prevails under dense vegetation (*7, 8*). This behavior may be crucial for success in the competition for light since, in fast-developing stands, individuals are likely to be rapidly suppressed if their mechanisms of "shade avoidance" begin to operate only after light availability has been severely reduced (*8*). We show that this early reaction to the presence of neighbors is triggered by low R:FR ratios received at the stem level and that this localized drop in the R:FR balance is mainly a consequence of the FR light reflected from nearby leaves.

The possibility that FR radiation reflected from neighboring plants may initiate shade-avoidance reactions before canopy closure was suggested by previous experiments in canopies of low leaf area index (LAI = leaf area per unit of soil area) (*7*). The strongest evidence for this hypothesis came from fiber optic studies showing large changes in the fluence rate of FR light inside the internodes in response to relatively small changes in canopy density (*9*). In the present experiments, seedlings of *Datura ferox* L. and *Sinapis alba* L. were grown in stands of different

Departamento de Ecología, Facultad de Agronomía, Universidad de Buenos Aires, Av. San Martín 4453, (1417) Buenos Aires, Argentina.

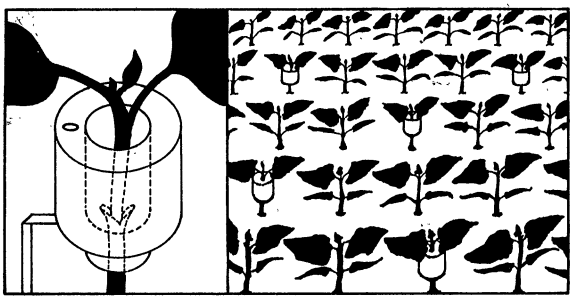

Fig. 1. Diagram showing the disposition of the annular filters and the arrangement of the seedlings in the experimental populations (*16*).

densities with their internodes surrounded by annular cuvettes containing $CuSO_4$ solutions (Fig. 1) that removed a large proportion of the FR component from the light received at the stem level (*10*). The key advantage of this approach is that we could maintain the R:FR ratio sensed by an internode constant and high over a range of canopy densities by adjusting the $CuSO_4$ concentration (Fig. 2).

The experiments were conducted in a greenhouse at the Faculty of Agronomy, Universidad de Buenos Aires (34°35'S, 58°29'W), under natural radiation. Seeds of *S. alba* (white mustard, Compañía Fanacoa, Argentina) and *D. ferox* (collected from plants invading soybean crops) were germinated and the seedlings planted in individual 500-cm^3 pots; other cultural practices were as described previously (*9*). The cuvettes were fitted around the seedlings when these were at the cotyledonary stage. After the primary leaves had begun to expand and when the first internode was about 8 to 12 mm high, the cotyledons were severed and the cuvettes were raised to cover the internodes completely. The seedlings were introduced into canopies 65 by 65 cm formed by plants of *S. alba* or *D. ferox* of the same height as treated individuals. The number of neighbors in each canopy was adjusted to obtain initial LAI values ranging from 0 to 0.85 (*11*). Then the cuvettes were filled with the appropriate $CuSO_4$ solution (see Fig. 2A) and, to provide control plants, we filled half of the cuvettes with water. In addition, some plants lacking cotyledons were introduced in the canopies without cuvettes. The duration of each experiment was 3 days (*D. ferox*) or 4 days (*S. alba*). The LAI of the canopies was checked daily (*11*), and the concentration of $CuSO_4$ in the filters was adjusted to maintain a constant R:FR ratio at the first internode level (Fig. 2A).

As in previous experiments (*7, 8*), first-internode elongation was strongly stimulated by a short exposure to an increased number of neighbors. Average promotion by a canopy of LAI in the range of 0.6 to 0.9 varied between 52 and 107% ($P < 0.001$). A similar response to plant density was measured for internodes surrounded by cuvettes filled with water (Fig. 3). Two striking features of the phenomenon are the rapidity of response and the relatively low LAI values required to stimulate elongation. Much of this reaction to the presence of neighbors was due to the perception by the stems of FR light scattered by leaves of adjacent plants. This is demonstrated by the markedly reduced effect of canopy density when internodes were covered by $CuSO_4$ filters (Fig. 3). These experiments provide direct evidence that elongation responses to plant density are photomorphogenetically controlled. Moreover, our results show that, in even-aged canopies, the R:FR ratio of the light that impinges laterally on the stems controls stem elongation well before the leaves are subjected to an important drop in light availability (see Fig. 3, A and C, triangles).

Interestingly, at LAI values greater than 1, $CuSO_4$ filters did not completely cancel the elongation response to plant density (Fig. 3, A, C, and D). At these LAI values the low R:FR ratio at the stem level is mainly a consequence of the reduced fluence rate of R light (*7*) (Fig. 2B), and the filters did not prevent the R:FR ratio from dropping slightly (~20%) below that measured for LAI = 0 (Fig. 2A). Although this reduction might be sufficient to stimulate elongation (*9, 12*), a possible direct effect of the lower fluence rate (*13*) cannot be ruled out. Moreover, at LAI >1 some leaves are shaded by neighboring plants (Fig. 3); therefore, perception of low R:FR ratios by leaves (*12, 14*), a better water status of the shoots in the densest stands, or both, might also have contributed to promote elongation.

More studies in real canopies are needed to understand how plants integrate the "light information" received by different organs and how this information interacts with other environmental signals. But the present experiments show that in canopies (or sites in the canopy) where mutual shading is low, internode elongation is locally modulated by the spectral light environment prevailing at the stem level. This finding calls attention to two important points. The first is that the spectra obtained with cosine-corrected planar sensors, which have been used almost universally to describe the radiation environment in canopies (*5, 15*), may

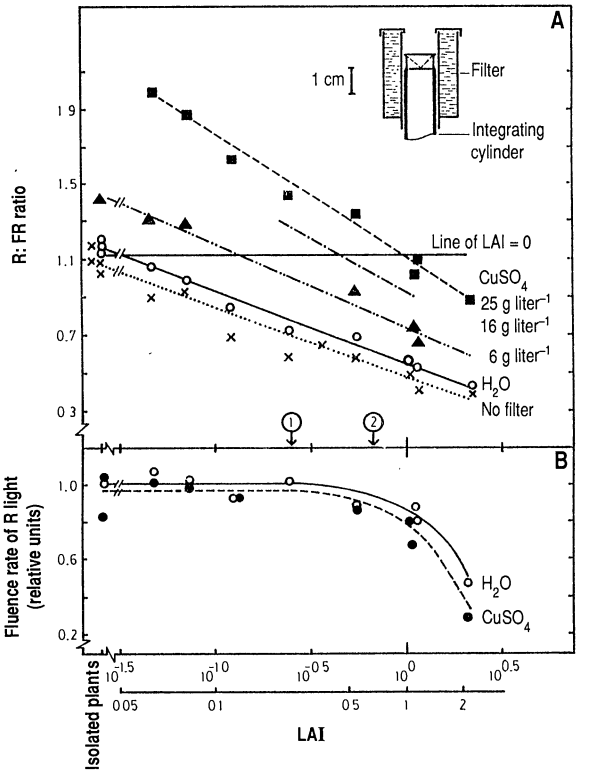

Fig. 2. (**A**) Relations between the R:FR ratio received at the first internode level and the LAI of the canopy for different concentrations of $CuSO_4$ in the filters. The solid line parallel to the abscissa is the average R:FR ratio received by internodes of isolated seedlings. To maintain a constant R:FR ratio during the experiments, we changed the $CuSO_4$ concentration from 6 to 16 g liter^{-1} and from 16 to 25 g liter^{-1} when canopy LAI exceeded values indicated by "1" and "2", respectively. (**B**) The effect of increasing LAI on the fluence rate of R light (650 nm) received by the internodes when they were surrounded by water (——) or $CuSO_4$ (- - - - -) filters. Results were normalized to the value for isolated plants surrounded by water filters. To construct the $CuSO_4$ curve, we selected the salt concentration according to canopy LAI as indicated in (A). R:FR determinations (650 nm:725 nm quantum flux ratio) were taken with an integrating-cylinder probe attached to an SR spectroradiometer (ISCO) (*17*). The probe was held inside the filters in the place of the internodes (see diagram at the upper-right corner). The different LAI values were obtained with combinations of seedling numbers and size. Measurements were made at midday (solar elevation ≥36°); clear sky.

not adequately reflect the light conditions at the photoreceptive site in even-aged populations (for example, crop stands). This is the reason why the R:FR–triggered responses reported here could not be predicted on the basis of classic spectroradiometer studies.

The second point is connected with the ecological significance of R:FR perception by plants. Our results indicate that, by sensing local modifications in the R:FR balance at the stem level, the elongating shoots may acquire information about their relative position in the stand at a very early stage of canopy development. This information may influence growth pattern and hence light interception in the near future. Thus, individual differences in the capacity to detect and react to localized changes in the R:FR ratio might determine quite different abilities to compete for light in rapidly growing populations.

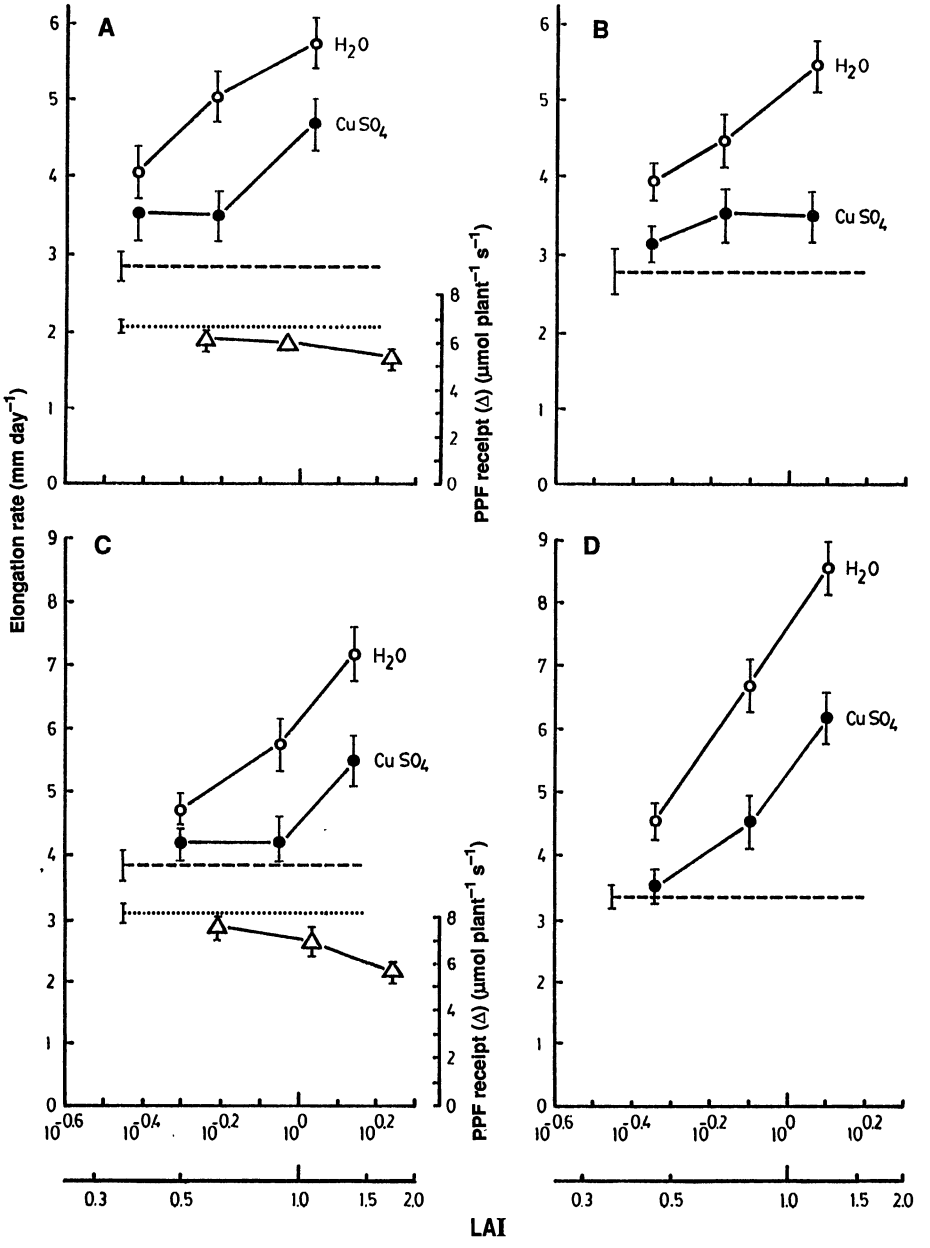

Fig. 3. Elongation of the first internode of *S. alba* (**A** and **B**) or *D. ferox* (**C** and **D**) seedlings when plants were exposed to background canopies of different LAI: (○) internodes surrounded by water filters; (●) internodes surrounded by $CuSO_4$ (FR-blocking) filters. Exposure times were 4 days (A and B) or 3 days (C and D). The dashed line is the extension rate of isolated seedlings with internodes covered by water filters (*18*). Also shown is the effect of canopy density on PPF intercepted per individual seedlings (△, PPF = photosynthetic photon flux, 400 to 700 nm). The dotted line represents PPF intercepted by isolated plants. Elongation rates were obtained from length measurements taken from the cotyledonary node to the first leaf node at the beginning and at the end of the treatment period. Each point is the average elongation of 17 plants (± 1 SE) plotted against the LAI estimated for the middle of the experimental period (*11*). PPF intercepted per seedling was estimated as follows. Five plants were randomly selected to represent each LAI treatment; PPF at the adaxial surface of each individual leaf was measured with a cosine-corrected sensor (LI-190SB, LI-COR) held at the same angle of display as the lamina; then the figures were integrated for the whole seedling on the basis of leaf area data (*8*). Peak levels of PPF at midday on a horizontal plane were >1300 μmol m^{-2} s^{-1} (A and B) or >1500 μmol m^{-2} s^{-1} (C and D). Photoperiod was 12.2 hours (A), 12.6 hours (B), 13.9 hours (C), and 14.3 hours (D).

REFERENCES AND NOTES

1. J. L. Harper, *Population Biology of Plants* (Academic Press, London, 1977).
2. E. I. Newman, in *Encyclopedia of Plant Physiology*, new series, O. L. Lange, P. S. Nobel, C. B. Osmond, H. Ziegler, Eds. (Springer-Verlag, Berlin, 1983), vol. 12C, pp. 679–710; J. L. Harper, in *Population Biology and Evolution of Clonal Organisms*, J. B. C. Jackson, L. W. Buss, R. E. Cook, Eds. (Yale Univ. Press, New Haven, CT, 1985), pp. 1–34.
3. N. J. Rosenberg, *Microclimate: The Biological Environment* (Wiley, New York, 1974); J. L. Monteith, Ed., *Vegetation and the Atmosphere* (Academic Press, London, 1976).
4. H. Smith, *Annu. Rev. Plant Physiol.* **33**, 481 (1982); ——— and D. C. Morgan, in *Encyclopedia of Plant Physiology*, new series, W. Shropshire, Jr., and H. Mohr, Eds. (Springer-Verlag, Berlin, 1983), vol. 16B, pp. 491–517.
5. P. E. Vézina and D. W. K. Boulter, *Can. J. Bot.* **44**, 1267 (1966); M. J. Kasperbauer, *Plant Physiol.* **47**, 775 (1971); M. G. Holmes and H. Smith, *Photochem. Photobiol.* **25**, 539 (1977).
6. D. C. Morgan and H. Smith, *Nature* **262**, 210 (1976); *Planta* **142**, 187 (1978); A. Lecharny and R. Jacques, *Plant Cell Environ.* **5**, 31 (1982); H. Smith and P. Hayward, *Photochem. Photobiol.* **42**, 685 (1985); R. Child and H. Smith, *Planta* **172**, 219 (1987).
7. C. L. Ballaré, R. A. Sánchez, A. L. Scopel, J. J. Casal, C. M. Ghersa, *Plant Cell Environ.* **10**, 551 (1987).
8. C. L. Ballaré, R. A. Sánchez, A. L. Scopel, C. M. Ghersa, *Oecologia (Berlin)* **76**, 288 (1988).
9. C. L. Ballaryé, A. L. Scopel, R. A. Sánchez, *Plant Physiol.* **89**, 1324 (1989).
10. Water solutions of $CuSO_4$ absorb strongly beyond 700 nm and have been used as primary filters to remove the FR and infrared radiation in growth chambers with artificial lighting [R. B. Withrow and L. Price, *Plant Physiol.* **28**, 105 (1953)]. There is little attenuation of visible-wavelength bands for short optical paths through dilute solutions.
11. Canopies were formed with plants growing in individual pots; different LAI values were obtained by changing the number of seedlings. We estimated LAI by using a nondestructive method based on measurements of leaf length and width (7).
12. D. C. Morgan, T. O'Brien, H. Smith, *Planta* **150**, 95 (1980).
13. R. Garrison and W. R. Briggs, *Bot. Gaz. (Chicago)* **133**, 270 (1972); A. Lecharny and R. Jacques, *Planta* **149**, 384 (1980).
14. R. Garrison and W. R. Briggs, *Bot. Gaz. (Chicago)* **136**, 353 (1975); A. Lecharny, *Planta* **145**, 405 (1979); J. J. Casal and H. Smith, *ibid.* **175**, 214 (1988).
15. M. J. Kasperbauer, P. G. Hunt, P. E. Sojka, *Physiol. Plant.* **61**, 549 (1984).
16. Internode temperature was continuously monitored during the experiments with NTC thermistors (type NTH2074A, Murata Manufacturing) inserted into the stems of some plants and connected to a LI-1000 datalogger, LI-COR. To avoid overheating of internodes surrounded by filters, we pumped cool and humid air into the stem-filter interspace at a rate of 40 ml s^{-1}, using 3.6-mm polyvinyl chloride tubes. Hourly averages of internode temperature in the $CuSO_4$ treatments were within ±1.5°C of the temperature of the water controls.
17. The integrating cylinder collects the light flux from all compass points parallel to the ground (7). This

component of global radiation makes a very minor contribution to the photons accepted by a horizontal, cosine-corrected receiver but plays an important role in determining the light environment within the axis (*9*).

18. The use of $CuSO_4$ (6 g liter^{-1}) filters did not significantly affect elongation of isolated seedlings ($P > 0.5$).
19. We thank O. E. Sala for critical reading of the manuscript. Supported by grants from the Consejo Nacional de Investigaciones Científicas y Técnicas and the University of Buenos Aires (AG 062).

6 July 1989; accepted 31 October 1989

Specific Expression of a Tyrosine Kinase Gene, *blk*, in B Lymphoid Cells

SUSAN M. DYMECKI, JOHN E. NIEDERHUBER, STEPHEN V. DESIDERIO

Several pathways of transmembrane signaling in lymphocytes involve protein-tyrosine phosphorylation. With the exception of p56^{lck}, a tyrosine kinase specific to T lymphoid cells that associates with the T cell transmembrane proteins CD4 and CD8, the kinases that function in these pathways are unknown. A murine lymphocyte complementary DNA that represents a new member of the *src* family has now been isolated and characterized. This complementary DNA, termed *blk* (for B lymphoid kinase), specifies a polypeptide of 55 kilodaltons that is related to, but distinct from, previously identified retroviral or cellular tyrosine kinases. The protein encoded by *blk* exhibits tyrosine kinase activity when expressed in bacterial cells. In the mouse and among cell lines, *blk* is specifically expressed in the B cell lineage. The tyrosine kinase encoded by *blk* may function in a signal transduction pathway that is restricted to B lymphoid cells.

THE PROGRAMS OF LYMPHOCYTE proliferation and differentiation that underlie the humoral immune response are mediated by the binding of specific antigens, cell-surface adhesion molecules, and lymphokines to receptors on B and T cells. Protein-tyrosine phosphorylation is implicated as being important in these processes. Stimulation of T cells by specific antigen results in tyrosine phosphorylation of specific substrates, including the zeta chain of the T cell receptor–CD3 complex (*1*). Likewise, within several minutes of exposure to interleukin-2 (IL-2), a number of proteins in responsive cells become phosphorylated on tyrosine residues; the concentration of IL-2 required for phosphorylation is similar to that required for proliferation (*2*). Interleukin-3, which exerts its effects on lymphoid and myeloid progenitor cells, also induces phosphorylation of specific substrates on tyrosine, including a 140-kD protein that may represent a component of the IL-3 receptor (*3*).

By analogy to the receptors for epidermal growth factor and insulin, some of the transmembrane proteins implicated in lymphocyte activation may exert their effects through specific tyrosine kinases. In the growth factor receptor kinases, ligand-binding and kinase domains are covalently linked (*4*). Such an association can also be achieved by noncovalent interactions. The *lck* gene, a member of the *src* family, is expressed predominantly in T lymphocytes (*5*). Its product, a 56-kD tyrosine kinase (p56^{lck}), is specifically associated with two transmembrane proteins implicated in T cell activation, CD4 and CD8; cross-linking of CD4 is accompanied by an increase in the protein-tyrosine kinase activity of p56^{lck} (*6*). Other lymphocyte transmembrane proteins may also couple to tyrosine kinases of the Src-type. Seven members of the *src* family have been described: *src, lyn, yes, fyn, fgr, hck*, and *lck* (*7, 8*). Of these, only *lck* is expressed predominantly in lymphoid cells. The participation of tyrosine phosphorylation in multiple pathways of signal transduction in B and T cells suggested the existence of additional, lymphoid-specific members of the *src* family.

The catalytic domains of Src-type tyrosine kinases are highly conserved (*7, 8*), suggesting that degenerate oligonucleotide probes could be used to identify genes encoding similar proteins. We compared the nucleotide sequences of four tyrosine kinase genes: *lck* (*5*), v-*abl* (*9*), c-*src* (*10*), and v-*yes* (*11*). Two regions of highly conserved nucleotide sequence were identified, and three degenerate oligonucleotides, complementary to the coding strand within these regions, were synthesized (*12*). A mixed B and T cell cDNA library was screened with a pool of these probes, and seven independent cDNA clones were isolated. On the basis of DNA hybridization, clones 54, 96, 100, 108, and 109 were uniquely represented in the set, whereas clones 102 and 103 appeared to be closely related. By nucleotide sequence, clones 54, 96, and 108 were found to represent *src, lck*, and *abl*, respectively (*13*). Clones 100 and 109 are likely to be murine homologs of *yes* and *fyn* because partial nucleotide sequence analysis revealed >95% identity with the human genes (*13*). The nucleotide sequences of clones 102 and 103 confirmed that they were overlapping cDNAs and indicated that they were derived from a new member of the *src* family, which we have called *blk*.

On rescreening the library with *blk* cDNA probes, three additional 5′ overlapping clones, designated 201, 205, and 215, were obtained. These five cDNA clones define a DNA sequence spanning 2094 bp. An open reading frame of 499 codons extends from a Met codon at nucleotides 350 to 352 to an amber stop codon at nucleotides 1847 to 1849 (Fig. 1). The Met codon at positions 350 to 352 occurs in a context favorable for translation (*14*). Four termination codons occur upstream from this Met codon in the same reading frame. Five other potential Met codons lie upstream from nucleotide 350, but these are followed by in-frame termination codons (Fig. 1A). Thus, the entire *blk* coding sequence is represented within the region included in the clones. The most 3′ terminal clone, 103, contains 245 bp of 3′ untranslated region and is devoid of a polyadenylated tract or a polyadenylation signal (*15*); it is likely that this clone does not include the complete 3′ untranslated sequence of *blk*.

To prove the integrity of the large open reading frame predicted by the nucleotide sequence, we synthesized *blk* transcripts in vitro, and translated them in a cell-free system (Fig. 2). The complete sense transcript directed the synthesis of a polypeptide of apparent molecular mass 55-kD, in agreement with the molecular mass predicted by the nucleotide sequence (Fig. 2B, lane 1). A truncated transcript that includes 314 codons of *blk* open reading frame and 6 additional codons derived from the bacterial cloning vector (Fig. 2A), directed the synthesis of a 33-kD polypeptide (Fig. 2B, lane 2), thus verifying that the major translation product is initiated at or near the Met codon at nucleotides 350 to 352. No polypeptides of comparable size were detected in reactions directed by antisense transcripts (Fig. 2B, lanes 3 and 4) or in reactions devoid of exogenous RNA (Fig. 2B, lane 5).

The protein encoded by *blk* (p55^{blk}) represents a new member of the Src family of

S. M. Dymecki and S. V. Desiderio, Department of Molecular Biology and Genetics, and the Howard Hughes Medical Institute Laboratory of Genetics, The Johns Hopkins University School of Medicine, Baltimore, MD 21205.
J. E. Niederhuber, Departments of Surgery, Oncology, and Molecular Biology and Genetics, The Johns Hopkins University School of Medicine, Baltimore, MD 21205.